J Electroceram (2009) 23:154–158
DOI 10.1007/s10832-007-9346-5

Investigation of microwave dielectric properties in the $BaO–Nb_2O_5–P_2O_5$ system

In-Sun Cho · Jeong Seop Lee · Shin-Tae Bae · Jeong-Ryeol Kim · Kug Sun Hong

Received: 1 June 2007 / Accepted: 10 October 2007 / Published online: 27 October 2007

Abstract $BaNb_2P_2O_{11}$ and $Ba_3Nb_2P_4O_{18}$ compounds with corner-sharing NbO_6 octahedra and PO_4 tetrahedra were prepared by a conventional solid-state reaction method. The crystal structure and microstructure were investigated by X-ray powder diffraction and field emission scanning electron microscope, respectively. The microwave dielectric properties were measured using a network analyzer. Both ceramics were sintered at a relatively low temperature of 1150 °C and had a relative density of ~96%. Compared to $Ba_3Nb_2P_4O_{18}$, $BaNb_2P_2O_{11}$ had a higher permittivity of 31.7. However, the quality factor of $BaNb_2P_2O_{11}$, was smaller than $Ba_3Nb_2P_4O_{18}$. Furthermore, the effect of the crystal structure on the microwave dielectric properties was investigated.

Keywords $BaO–Nb_2O_5–P_2O_5$ · Dielectric properties · $BaNb_2P_2O_{11}$ · $Ba_3Nb_2P_4O_{18}$ · Bond strength

1 Introduction

Recently, many investigations on developing dielectric materials for resonators at microwave frequencies have been performed due to fast growth of mobile communication systems such as global positioning systems (GPS) and personal communication systems (PCS). Microwave dielectric materials are separated into two groups according to dielectric properties. One group is characterized by low permittivity and a high quality factor, such as Al_2O_3, phosphates and $Ba(Mg_{1/2}Ta_{2/3})O_3$ [1–3]. The other group is represented by high permittivity and moderate quality factor, such as TiO_2, $BaO–Nd_2O_3–TiO_2$ and $BaO–TiO_2–Nb_2O_5$ systems [4–7].

Among various dielectric compositions, complex perovskite compounds such as $Ba(Mg_{1/3}Ta_{2/3})O_3$ and $Ba(Zn_{1/3}Ta_{2/3})O_3$ are known to have the best microwave dielectric properties for future trends [8–10]. However, research focused on discovering new compositions is still active as there is a great demand for a variety of permittivity, low cost, and low firing conditions.

Within the $BaO–Nb_2O_5–P_2O_5$ system, the crystal structures of $BaNb_2P_2O_{11}$ and $Ba_3Nb_2P_4O_{18}$ have been individually reported by Murashova et al. and Wang et al. [11, 12]. Both compounds contain corner-sharing NbO_6 octahedra and PO_4 tetrahedra. In the $BaNb_2P_2O_{11}$ structure, each NbO_6 octahedron shares corner oxygen atoms with three NbO_6 octahedra and three PO_4 tetraheda. Alternatively, $Ba_3Nb_2P_4O_{18}$ is composed of NbO_6 octahedra connected to five PO_4 tetrahedra. The crystal structure parameters are listed in detail in Table 1.

In the present study, the microwave dielectric properties of $BaNb_2P_2O_{11}$ and $Ba_3Nb_2P_4O_{18}$ were investigated, and the effect of crystal structure on their microwave dielectric properties were examined with respect to the bond strength and covalence.

2 Experiments

$BaNb_2P_2O_{11}$ and $Ba_3Nb_2P_4O_{18}$ powders were prepared using a conventional solid-state reaction method. $BaCO_3$ (99.9%, Cerac, USA), Nb_2O_5 (99.9%, High Purity Chemicals, Japan) and $(NH_4)_2HPO_4$ (99%, Junsei, Japan) were

I.-S. Cho · J. S. Lee · S.-T. Bae · K. S. Hong (✉)
School of Materials Science & Engineering,
College of Engineering, Seoul National University,
Shillim-dong, San 56-1,Gwanak-gu,
Seoul 151-744, South Korea
e-mail: kshongss@plaza.snu.ac.kr

J.-R. Kim
168 Materials Research Lab., Penn State University,
University Park, PA 16802, USA

Table 1 Crystal structure parameters of $BaNb_2P_2O_{11}$ and $Ba_3Nb_2P_4O_{18}$.

Compound	Unit cell parameter							Space group	Z	ρth (g/cm^3)
	a (Å)	b (Å)	c (Å)	α (°)	β (°)	γ (°)	V_{cell} (Å^3)			
$BaNb_2P_2O_{11}$	5.072	5.072	59.1		90		1,316.67	R3-c	6	4.246
$Ba_3Nb_2P_4O_{18}$	4.8898	9.076	9.521	88.815	78.638	78.491	405.84	P1-	1	4.13

used as raw materials. Stoichiometric mixtures of the starting materials were ball milled with ZrO_2 media in ethanol for 24 h and calcined at 1100 °C for 4 h. The calcined powders were milled again and uniaxially pressed into pellets at a pressure of 1000 kg/cm^2. The pellets were sintered at 1000–1200 °C for 2 h using a heating rate of 5 °C/min.

The phases in the calcined and sintered samples were identified using an X-ray powder diffractometer (XRD, Model M18XHF, Mac-science Instruments, Japan). The microstructures of the sintered samples were examined using a field-emission scanning electron microscope (FE-SEM; Model JSM-6330F, JEOL, Japan). The bulk density of the sintered samples was determined by Archimedes' method.

The high-frequency dielectric properties of the sintered samples were measured using an HP 8720C network analyzer. The quality factor ($Q\times f$) was measured by the transmission cavity method using a Cu cavity and Teflon supporter [13]. The permittivity (ε_r) was measured using the post resonator method and the temperature coefficient of the resonant frequency (τ_f) was measured using an Invar cavity in the temperature range of 20 to 80 °C [14, 15]. The temperature dependence of permittivity was measured using an HP 4194A impedance/gain phase analyzer in the temperature range of −120 to 90 °C.

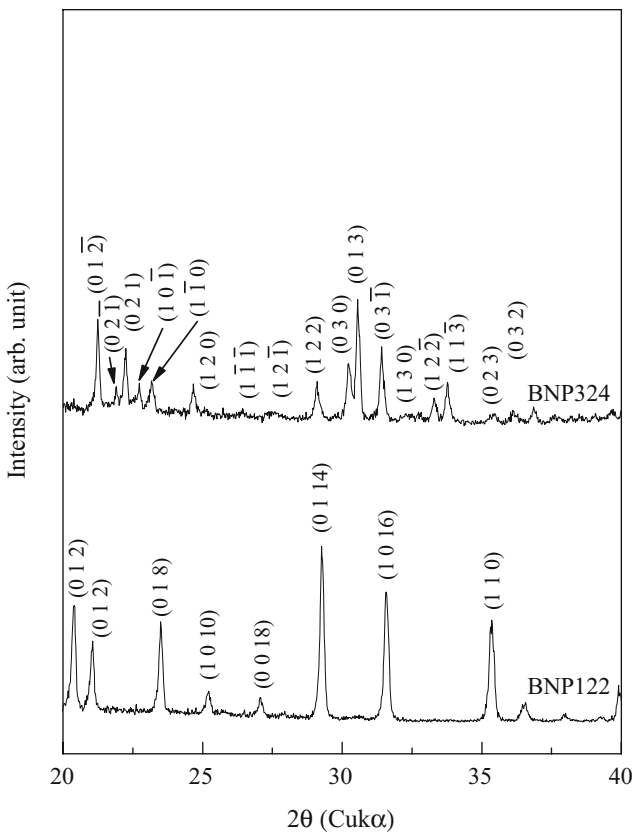

Fig. 1 XRD patterns of $BaNb_2P_2O_{11}$ and $Ba_3Nb_2P_4O_{18}$ calcined at 1100 °C for 4 h

3 Results and discussion

Figure 1 shows the XRD patterns of $BaNb_2P_2O_{11}$ [BNP122] and $Ba_3Nb_2P_4O_{18}$ [BNP324] powders calcined at 1000 °C for 4 h, which were corroborates earlier reports and reasonably indexed the BNP122 and BNP324 single phase, respectively [11, 12].

By using these powders, the sintering properties and microstructures were investigated. As shown in Fig. 2, the relative density of BNP122 linearly increased from 87 to 96.2% with increasing sintering temperature. However, for BNP324, the relative density rapidly increased with increasing sintering temperature, reaching saturation at 1150 °C. Furthermore, the BNP324 sample melted when the sintering temperature increased from 1150 to 1200 °C.

Figure 3 shows the microstructures of the BNP122 and BNP324 samples sintered at various temperatures. BNP324 sample sintered at 1050 °C had a porous microstructure with

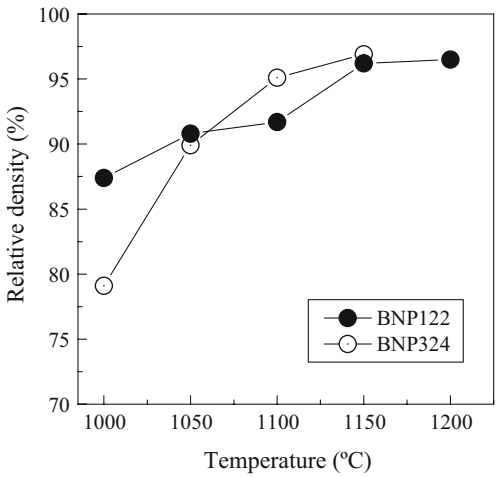

Fig. 2 Relative densities of $BaNb_2P_2O_{11}$ and $Ba_3Nb_2P_4O_{18}$ versus the sintering temperature

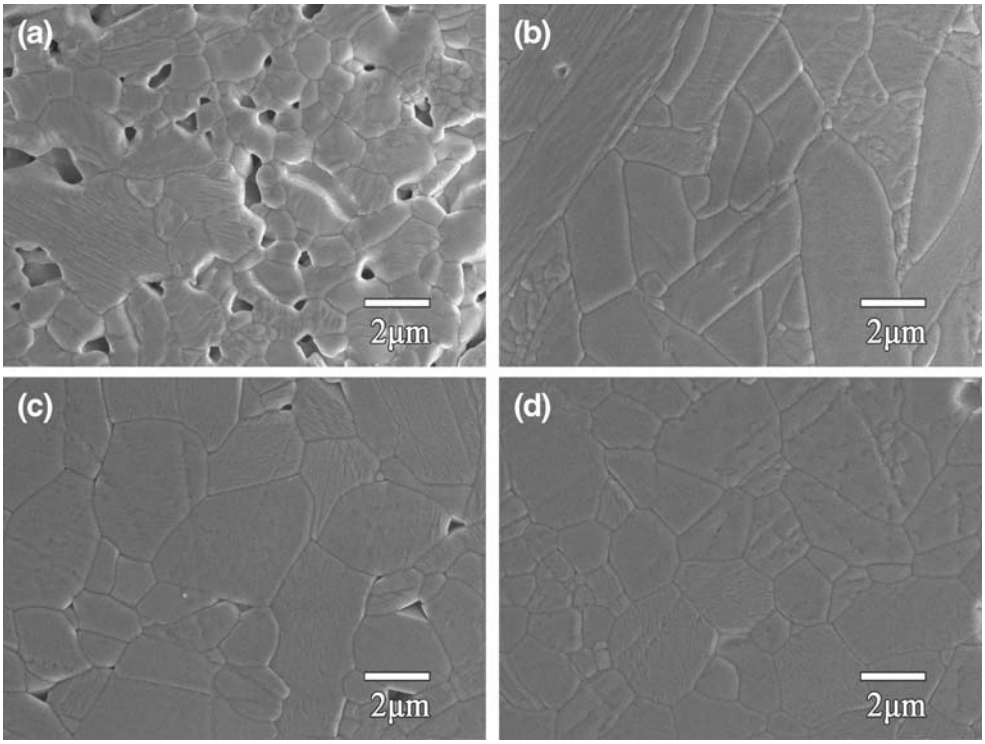

Fig. 3 Microstructures of $Ba_3Nb_2P_4O_{18}$ sintered at (**a**) 1050 °C, (**b**) 1150 °C, and $BaNb_2P_2O_{11}$ sintered at (**c**) 1150, and 1200 °C

equiaxed, 1–3 μm grains. However, upon increasing the sintering temperature from 1050 to 1150 °C, grain growth and elongated grains were observed as shown in Fig. 3(b).

Alternatively, the BNP122 samples sintered at 1150 °C had a dense microstructure with equiaxed, 2–4 μm grains. Grain growth and elongated grains were not observed when the sintering temperature increased to 1200 °C.

The microwave dielectric properties of the sintered samples are shown in Table 2. The calculated permittivity ($\varepsilon_{r,\ cal}$) was obtained from the Clausius–Mossotti equation;

$$\varepsilon_{r,\mathrm{cal}} = (3V_\mathrm{m} + 8\pi\alpha_D)/(3V_\mathrm{m} - 4\pi\alpha_D) \quad (1)$$

where, V_m is the molar volume and α_D is the sum of ionic polarizability given by Shannon [16].

The calculated permittivity of BNP122 and BNP324 were 9.6 and 8.1, respectively. Both compounds exhibited similar low permittivity values, however the measured permittivity of BNP122 (31.7) was much greater than BNP324 (10.0).

To understand the difference between the measured permittivity values, the crystal structures were investigated. According to Murashova et al. and Wang et al., both $BaNb_2P_2O_{11}$ and $Ba_3Nb_2P_4O_{18}$ had corner-sharing NbO_6 octahedra and PO_4 tetrahedra. However, the linkage between the NbO_6 octahedra and PO_4 tetrahedra were quite different.

On the basis of the refined crystal structure parameters and bond valence theory, the bond strength and covalence of the cation-oxygen were determined using the following equations [17, 18];

$$V_{ij} = \sum\nolimits_j S_{ij} \quad (2)$$

$$S_{ij} = \exp\left[\left(R_{ij} - d_{ij}\right)/b\right] \quad (3)$$

$$f_c = aS_{ij}^M \quad (4)$$

where R_{ij} is the bond valence parameter, d_{ij} is the bond length and b is the universal constant, 0.37 Å. Additionally, f_c is the covalence, a and M in Eq. 4 are empirically determined parameters and depend on the number of core

Table 2 The microwave dielectric properties of the $BaNb_2P_2O_{11}$ and $Ba_3Nb_2P_4O_{18}$.

Compound	Sintering temperature (°C)	Relative density (g/cm^3)	$\varepsilon_{r,\ cal}$	$\varepsilon_{r,\ mea}$	$Q\times f$ (GHz)	τ_f (ppm/°C)
$BaNb_2P_2O_{11}$	1150	96.2	9.6	31.8	24,100	+44.9
	1200	96.5		31.7	23,800	+53.1
$Ba_3Nb_2P_4O_{18}$	1100	95.1	8.1	10.1	51,000	−34.2
	1150	96.9		10.0	58,400	−33.5

Table 3 Bond valence sum, average bond strength and covalence of Ba–O, Nb–O, P–O bonds in $BaNb_2P_2O_{11}$ and $Ba_3Nb_2P_4O_{18}$.

	Bond valence sum[a]					Average bond strength			Covalence (v. u)[b]		
	V_{Ba1-O}	V_{Ba2-O}	V_{Nb-O}	V_{P1-O}	V_{P2-O}	$<S_{Ba-O}>$	$<S_{Nb-O}>$	$<S_{P-O}>$	$f_{c,\ Ba-O}$	$f_{c,\ Nb-O}$	$f_{c,\ P-O}$
BNP122	1.791 (12)	–	5.213 (6)	5.032 (4)	–	0.149	0.869	1.258	0.025 (27.4%)	0.393 (62.6%)	0.787 (67.3%)
BNP324	1.849 (10)	1.826 (10)	5.228 (6)	5.032 (4)	5.031 (4)	0.184	0.871	1.258	0.034 (32.4%)	0.395 (62.7)	0.787 (67.3%)

[a] The coordination numbers are shown in parenthesis.
[b] The percentage covalencies were shown in parentheses.

electrons in the cation. Previously reported values for the bond valence parameters were used [19].

The calculated bond valence sum, average bond strength and covalence of Ba–O, Nb–O, P–O bonds in $BaNb_2P_2O_{11}$ and $Ba_3Nb_2P_4O_{18}$ are shown in Table 3. The average bond strength can be calculated by the average bond valence sum divided by the average cation coordination numbers. The average bond strength and covalence of the Nb–O and P–O bonds in both compounds were similar, whereas the Ba–O bond was quite different. The average bond strength and covalence of the Ba–O bond in the BNP122 were much smaller than BNP324, which indicated the Ba–O bond of BNP122 exhibited more ionic character (72.6%).

In the microwave frequency region, ionic polarizability is the main contributor to permittivity as the electronic polarizability is much smaller. The ionic polarizability occurs from opposite displacements of the cation and anion under applied electric field and is known to be related to the bond strength, or in other words, the bond length between the cation and anion [20].

Guo et al. suggested the permittivity differences between $Sr(Al_{1/2}Nb_{1/2})O_3$ and $Sr(Al_{1/2}Ta_{1/2})O_3$ is due to variations in the bond strength of Nb–O and Ta–O [21]. Hence, it may be concluded that the difference is attributed to the difference of bonding character. As a result, the smaller bond strength and larger ionic character of Ba–O influenced the higher permittivity of BNP122.

The $Q\times f$ value of the BNP122 sample was smaller than the BNP324 sample. It is well known that losses in microwave dielectrics are intrinsic and extrinsic. The intrinsic loss is related to the crystal structure and bonding character of the materials, and the extrinsic loss is mainly related to defects, grain size and porosity [22].

It is believed that the effect of the extrinsic loss is small, as the relative densities and microstructures of both compounds were analogous. Therefore, the smaller $Q\times f$ value of the BNP122 sample mainly originated from intrinsic factors.

According to the classic dielectric dispersion theory, intrinsic dielectric losses are mainly related to the anharmonicity of optical lattice vibration modes, which usually can be modeled as an additive system of damped harmonic oscillators [23]. A larger the force constant implies a lower damping constant, that is, a lower dielectric loss.

The covalence of Nb–O (~62%) and P–O bonds (~67%) was similar in both compounds; whereas Ba–O in BNP122 and BNP324 exhibited 72.6% and 67.6% ionic character, respectively. Therefore, as discussed above, the greater ionic character of the Ba–O bond was responsible for the smaller $Q\times f$ value in BNP122.

The τ_f value is related to the temperature coefficient of the permittivity (τ_ε) and the linear thermal expansion coefficient (α_L) by $\tau_f = 1/2\tau_\varepsilon - \alpha_L$. Figure 4 shows temperature dependence of permittivity at 1 MHz for BNP122 and BNP324. The τ_ε value of BNP122 and BNP324 were −91.7 and 46.9 ppm/°C, respectively.

Low permittivity materials typically have a positive τ_ε value and high permittivity materials (>20) generally have a more negative value [24]. Wise et al. proposed the ion coordination number and bonding character are the main sources of the difference in τ_f [25]. Additionally, Lufaso et al. reported lower valence and more underbonded (smaller bond valence sum) ions influence a more negative τ_f value in the perovskite system [26]. However, the results of this study exhibited a different trend. The BNP122, with more underbonded Ba–O, exhibited a more positive τ_f value (+53.1 ppm/°C). Therefore, to understand the difference

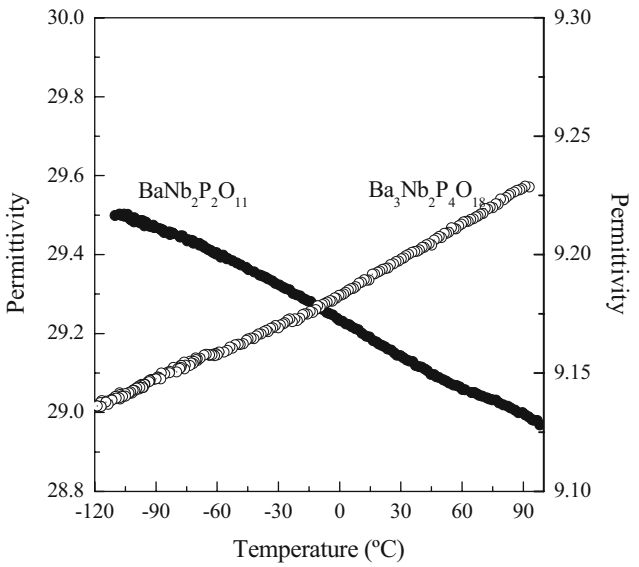

Fig. 4 Temperature-dependence of permittivity at 1 MHz for $BaNb_2P_2O_{11}$ and $Ba_3Nb_2P_4O_{18}$

between the τ_f value and crystal structure in the BaO–Nb_2O_5–P_2O_5 system, further analyses are needed.

4 Conclusion

$BaNb_2P_2O_{11}$ and $Ba_3Nb_2P_4O_{18}$ compounds with corner-sharing NbO_6 octahedra and PO_4 tetrahedra were prepared by a conventional solid-state reaction method. Both compounds were sintered at 1150–1200 °C and exhibited dense microstructures. The microwave dielectric properties of the sintered samples were investigated and the effect of the crystal structure was examined. On the basis of the refined crystal structure parameters and bond valence theory, the bond strength and covalence of the cation-oxygen were determined. The differences of the permittivity, $Q\times f$ and τ_f values in both compounds were attributed to the bonding character of Ba–O. The bond strength and covalency of Ba–O in the $BaNb_2P_2O_{11}$ were smaller than $Ba_3Nb_2P_4O_{18}$, which led to increased ionicity, and consequently increases permittivity. Additionally, the smaller $Q\times f$ and more positive τ_f of $BaNb_2P_2O_{11}$ were related to the ionic character of Ba–O. The $BaNb_2P_2O_{11}$ exhibited good microwave dielectric properties; ε_r=31.7, $Q\times f$=23,800 GHz and τ_f=+53.1 ppm/°C.

Acknowledgements This work was supported Korea Research Foundation Grant No. KRF-2002-041-D00259.

References

1. N.M. Alford, S.J. Penn, J. Appl. Phys. **80**, 5895 (1996)
2. I.-S. Cho, J.-R. Kim, D.-W. Kim, K.S. Hong, J. Electroceram. **16**, 379 (2006)
3. H. Tamura, T. Konoike, Y. Sakabe, K. Wakino, J. Am. Ceram. Soc. **67**, C-59 (1984)
4. S.B. Cohn, IEEE Trans. Microwave Theor. Tech. **16**, 218 (1968)
5. D. Kolar, S. Gabrscek, B. Volavsek, H.S. Parker, R.S. Roth, J. Solid State Chem. **38**, 158 (1981)
6. S. Solomon, M. Kumar, K.P. Surendran, M.T. Sebastian, P. Mohanan, Mater. Chem. Phys. **67**, 291 (2001)
7. I.-S. Cho, J.-R. Kim, D. W. Kim, D.-W. Kim, K.S. Hong, J. Euro. Ceram. Soc. **27**, 3081 (2007)
8. K. Matsumoto, T. Hiuga, K. Takada, H. Ichimura, IEEE Trans. Ultrason. Ferroelectr. Freq. Control **33**, 802 (1986)
9. S. Kawashima, M. Nishida, I. Ueda, H. Ouchi, J. Am. Ceram. Soc. **66**, 241 (1983)
10. Y.C. Chen, H.F. Cheng, C.C. Lee, C.T. Chia, H.L. Liu, I.N. Lin, J. Electroceram. **13**, 271 (2004)
11. E.V. Murashova, V.K. Trunov, Y.A. Velikodnyi, Russ. J. Inor. Chem. **31**, 951 (1986)
12. X. Wang, L. Liu, A.J. Jacobson, J. Mater. Chem. **10**, 2774 (2000)
13. D. Kaifez, P. Guillion, *Dielectric Resonators*, (Artech House, Dedham, MA, 1986), p. 327
14. B.W. Hakki, P.D. Coleman, IEEE. Trans. Microw. Theory Tech. **8**, 402 (1960)
15. T. Nishikawa, K. Wakino, H. Tamura, H. Tanaka, Y. Ishikawa, IEEE MTT-S Dig. **3**, 277 (1987)
16. R.D. Shannon, J. Appl. Phys. **73**, 348 (1993)
17. I.D. Brown, Acta Cryst. B. **48**, 553 (1992)
18. I.D. Brown, R.D. Shannon, Acta Cryst. A. **29**, 266 (1973)
19. N.E. Bresea, M. O'Keeffe, Acta Cryst. B. **47**, 192 (1991)
20. A.R. West, *Solid State Chemistry and Its Applications*, (John Wiley & Sons, New York, 1984)
21. R. Guo, A.S. Bhalla, J. Sheen, F.W. Ainger, S. Erdei, E.S. Subbarao, L.E. Cross, J. Mater. Res. **10**, 18 (1995)
22. K. Wakino, H. Tamura, Ceram. Trans. **8**, 305 (1990)
23. W. Cochran, *The Dynamics of Atoms in Crystals*, (Edward Arnold, London, 1973), p. 101
24. A.G. Cockbain, P.J. Harrop, Br. J. Appl. Phys. D. **1**, 1109 (1968)
25. P.L. Wise, I.M. Reaney, W.E. Lee, D.M. Iddles, D.S. Cannell, T.J. Price, J. Mater. Res. **17**, 2033 (2002)
26. M.W. Lufaso, Chem. Mater. **16**, 2148 (2004)